Available online at www.sciencedirect.com

SCIENCE DIRECT®

Physica B 371 (2006) 107–111

PHYSICA B

www.elsevier.com/locate/physb

Electronic band structure pseudopotential calculation of wurtzite III-nitride materials

B. Rezaei, A. Asgari*, M. Kalafi

Research Institute for Applied Physics, Tabriz University, Tabriz 51665-163, Iran

Received 12 January 2005; received in revised form 16 August 2005; accepted 11 October 2005

Abstract

The electronic properties of the wurtzite III-nitride compound semiconductors GaN, InN and AlN are studied within the empirical pseudopotential approach. An analytical function for both symmetric and antisymmetric parts of the pseudopotential with adjustable coefficients has been reported. Using this model the selected features of these materials such as energy gap, bandwidth, crystal-field splitting energy, Luttinger-like parameters, and effective masses are calculated and compared to experimental and recently published theoretical results and the comparisons show a good agreement.

PACS: 71.15.Ap; 71.15.Dx

Keywords: GaN; InN; AlN; Band structures

1. Introduction

The great interest in III-nitride material system can be attributed to the promising electrical and optical properties of the binary compounds GaN, InN and AlN and their alloys. These binary compounds usually crystallize in the wurtzite structure [1,2]. Because of some prominent properties like strong piezoelectric polarization effect, wide band gap, high saturate electron drift velocity, high breakdown electric-field strength, and thermodynamically more stable, these materials are ideal for construction of blue/green light-emitting devices. Also they are attractive for use in field effect transistors indicated to operate at high power and/or temperature [3,4].

So, for III-nitride-based device design and optimization, one has to know exact band structure details and transport parameters. Presently, there are a number of band structure calculations ranging from phenomenological methods such as the k.p theory to atomistic ab initio methods, such as the self-consistent full-potential linear-augmented plane-wave method (FPLAPW) within local-density approximation (LDA), first-principles total-energy calculation, and pseudopotential methods, or more empirical methods such as the empirical pseudopotential method (EPM) [5–15].

In this theoretical study, the detailed electronic band structure calculation for wurtzite III-nitride materials by EPM method has been reported, and an analytical function was constructed using fitting procedure for both symmetric and antisymmetric parts of potential in Section 2. In Section 3 the most important band structure parameters such as effective mass parameters, A_i, describing the heavy-hole (hh), the light-hole (lh) and the crystal-field split-hole (ch) bands, were obtained from our calculations and they agree with last experimental data and recent theoretical results.

2. Model description

The binary compounds GaN, InN and AlN have been the subject of extensive theoretical studies in the last years. Their electronic structures have been studied with several different methods [5–8]. All of these methods give reliable

---

*Corresponding author. Tel.: +984113342564; fax: +984113347050.
E-mail address: asgari@ee.uwa.edu.au (A. Asgari).

0921-4526/$ - see front matter © 2005 Published by Elsevier B.V.
doi:10.1016/j.physb.2005.10.003

valence band structure but the band gaps are significantly underestimated.

Some electronic structure computations have also used the local EPM [9–15]. Obviously the EPM method cannot replace ab initio techniques, but it is simpler, computationally efficient, and the electronic structures obtained from the EPM can be optimized in order to closely match experimental and/or ab initio results.

At the present work the EPM electronic band structure as well as corresponding set of k.p parameters for (Ga, In and Al) N wurtzite crystals have been studied. The pseudopotential Hamiltonian used for our calculation is given by

$$H = -\vec{\nabla}^2 + V^{\mathrm{PS}}(\vec{r}), \tag{1}$$

where V^{PS} is the pseudopotential that can be expanded in reciprocal lattice vectors $\vec{G}$ as:

$$V^{\mathrm{PS}}(\vec{r}) = \sum_{\vec{G}} V(\vec{G})\mathrm{e}^{\mathrm{i}\vec{G}\cdot\vec{r}}. \tag{2}$$

For the wurtzite structures the matrix elements of the crystal pseudopotential in the spin-free pseudopotential Hamiltonian appears as [16]

$$\begin{aligned} V(\vec{G}-\vec{G}') = {} & V^{\mathrm{S}}(|\vec{G}-\vec{G}'|^2)S^{\mathrm{S}}(\vec{G}-\vec{G}') \\ & + \mathrm{i}V^{\mathrm{A}}(|\vec{G}-\vec{G}'|^2)S^{\mathrm{A}}(\vec{G}-\vec{G}') \end{aligned} \tag{3}$$

where V^{S} and V^{A} are the symmetric and antisymmetric form factors, and S^{S} and S^{A} are the symmetric and antisymmetric structure factors specific to the wurtzite crystals, respectively.

In the present calculation a suitable analytical expression for the atomic pseudopotential form factors of the III-nitrides binary compounds has been used, based on state-of-the-art knowledge of the band structure characteristics [10,12,15]. This expression, describing the symmetric, V^{S}, and antisymmetric, V^{A}, depends on a set of adjustable parameters that are determined by suitable fitting procedure and is given by

$$V^{\mathrm{S,A}} = \frac{a_1(q^2-a_2)}{1+\exp(a_3(q^2-a_4))}, \tag{4}$$

where q is the wave vector and a_i $(i = 1, \ldots, 4)$ are the fitting parameters.

Table 1
Equilibrium lattice and internal structural parameters for III-nitride materials

	a (Å)	c (Å)	u
GaN	3.19 [17]	5.189 [17]	0.377 [19]
InN	3.544 [18]	5.718 [18]	0.38 [19]
AlN	3.11 [17]	4.98 [17]	0.38 [19]

Using the lattice constants and internal structural parameters listed in Table 1, the fitting parameters for GaN, InN and AlN have been obtained and are listed in Table 2.

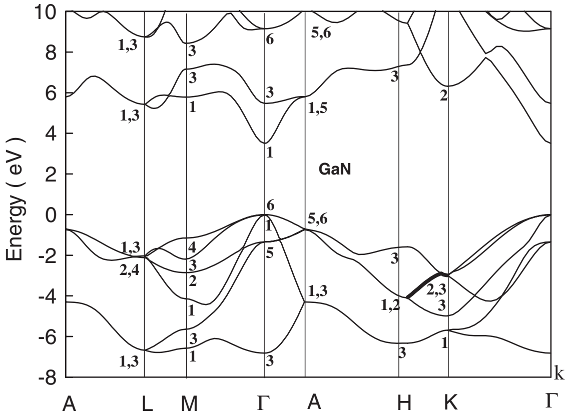

Fig. 1. Band structure of wurtzite GaN.

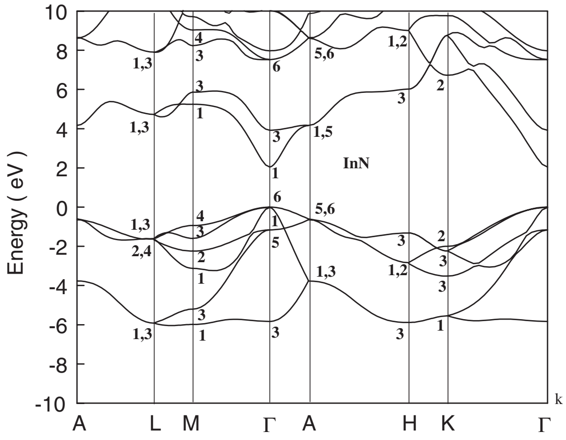

Fig. 2. Band structure of wurtzite InN.

Table 2
Fitting parameters of the analytical form factors of III-nitrides as defined in Eq. (4)

	V^{S}				V^{A}			
	a_1	a_2	a_3	a_4	a_1	a_2	a_3	a_4
GaN	0.04312	13.07859	0.28287	20.39298	0.51135	−20.12182	0.08350	−41.55743
InN	0.05310	11.50511	0.36895	16.44795	0.0167	−31.78	0.05278	−18.19
AlN	0.03695	11.95985	0.23356	22.23273	0.03225	−145.212	0.0947	−19.16

3. Results and discussions

The spin-free pseudopotentials obtained from the above fitting procedure were then used to predict the full band structure. The calculated full band structures for GaN, InN and AlN are shown in Figs. 1–3. To ensure the semi-empirical results accuracy in comparison with experimental data and other theoretical works, the band gaps and other known energy gaps for III-nitrides are shown in Table 3. Also, spin–orbit interaction is considered with the addition of the following spin–orbit matrix elements to the pseudopotential Hamiltonian as [14]

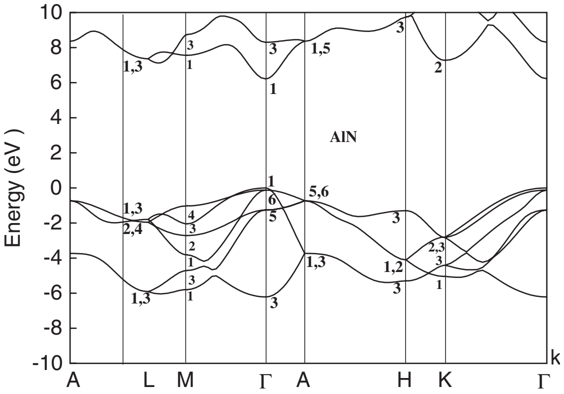

Fig. 3. Band structure of wurtzite AlN.

$$H^{\mathrm{SO}}_{\vec{G},\vec{G}'}(\vec{k}) = (\vec{K} \times \vec{K}').\vec{\sigma}_{s,s'}\{-\mathrm{i}\lambda^{\mathrm{S}} S^{\mathrm{S}}(\vec{G} - \vec{G}') + \lambda^{\mathrm{A}} S^{\mathrm{A}}(\vec{G} - \vec{G}')\}, \tag{5}$$

where $\vec{K} = \vec{k} + \vec{G}$, $\vec{K}' = \vec{k} + \vec{G}'$, and$\sigma_{s,s'} = \pm 1$ are the Pauli spin states. λ^{S} and λ^{A} are the symmetric and antisymmetric contributions to the spin–orbit Hamiltonian which are treated as adjustable parameters to give the correct spin splitting of valence band, Δ_{SO}, at the Γ-point [30]. The calculated values of λ^{S}, λ^{A} and also Δ_{SO} together with other published results are shown in Table 4 for wurtzite GaN, InN and AlN.

Table 3
Comparison of eigenenergies of GaN, InN and AlN with experimental and theoretical results (in eV)

	GaN				InN				AlN			
	Current work	Exp.	[10]	[15]	Current work	Exp.	[10]	[15]	Current work	Exp.	[10]	[15]
$\Gamma_1^c - \Gamma_6^v$	3.5036	3.6 [20], 3.44 [21], 3.5 [22]	3.5	3.47	2.0431	1.89 [25], 2.05 [26], 2.11 [18]	2.0527	2.59	6.2196	6.2 [27], 6.28[28]	5.8369	6.11
$\Gamma_6^v - \Gamma_1^v$	0.021	0.022 [23]	0.042	0.023	0.0214		0.0355	0.084	−0.1255		−0.1989	−0.16
$\Gamma_6^v - \Gamma_3^v$	6.816	7 [24]	8	6.94	5.8306		5.9719	5.50	6.2136	6 [29]	7.0061	6.41

Table 4
Comparison of spin-orbit splitting with other theoretical results

	λ^{S}(eV)	λ^{A}(eV)	Δ_{SO}(eV)		
			Current work	[12]	[31]
GaN	0.0002	0.00019	0.0096	0.011	0.013
InN	0.00025	0.00017	0.0139	0.011	0.001
AlN	0.00023	0.000191	0.018	0.011	0.019

Table 5
Valence band effective-mass parameters of GaN, InN and AlN

	Current work	GaN			Current work	InN			Current work	AlN	
		[12]	[14]	[15]		[12]	[14]	[15]		[12]	[15]
A_1	−7.22	−6.90	−7.24	−7.698	−9.64	−8.21	−9.28	−7.298	−4.38	−4.17	−4.794
A_2	−0.51	−0.73	−0.51	−0.6	−0.59	−0.68	−0.6	−0.441	−0.472	−0.58	−0.571
A_3	6.53	6.11	6.73	7.2	8.922	7.57	8.68	6.896	3.87	3.68	4.374
A_4	−2.8	−4.19	−3.36	−2.816	−3.92	−5.23	−4.34	−3.064	−1.62	−2.17	−1.484
A_5	−2.65	−3.94	−3.35	−2.971	−3.8	−5.11	−4.32	−3.12	−1.72	−2.27	−1.726
A_6	−3.54	−5.96	−4.72	−3.312	−5.3	−5.96	−6.08	−3.948	−2.16	−2.21	−1.788

Table 6
The electron and heavy (hh), light (lh) and crystal-field split (ch) hole effective masses for GaN, InN and AlN

	Current work	GaN			Current work	InN			Current work	AlN	
		[12]	[14]	[15]		[12]	[14]	[15]		[12]	[15]
$m_e^{\parallel}$	0.16	0.16	0.19	0.138	0.12	0.14	0.11	0.137	0.28	0.27	0.232
$m_{hh}^{\parallel}$	1.45	1.27	1.96	2.007	1.39	1.56	1.67	2.493	1.96	2.04	2.382
$m_{lh}^{\parallel}$	1.45	1.27	1.96	2.007	1.39	1.56	1.67	2.493	1.96	2.04	2.382
$m_{ch}^{\parallel}$	0.14	0.14	0.14	0.13	0.1	0.12	0.1	0.137	0.23	0.24	0.209
$m_e^{\perp}$	0.13	0.12	0.17	0.151	0.11	0.1	0.1	0.14	0.27	0.18	0.242
$m_{hh}^{\perp}$	1.52	1.02	1.87	2.249	1.41	1.25	1.61	2.599	2.68	2.08	3.04
$m_{lh}^{\perp}$	0.168	0.11	0.14	0.261	0.12	0.09	0.11	0.157	0.26	0.2	0.287
$m_{ch}^{\perp}$	1.96	1.36	1.96	0.317	1.69	1.46	1.67	1.446	2.12	1.71	1.157

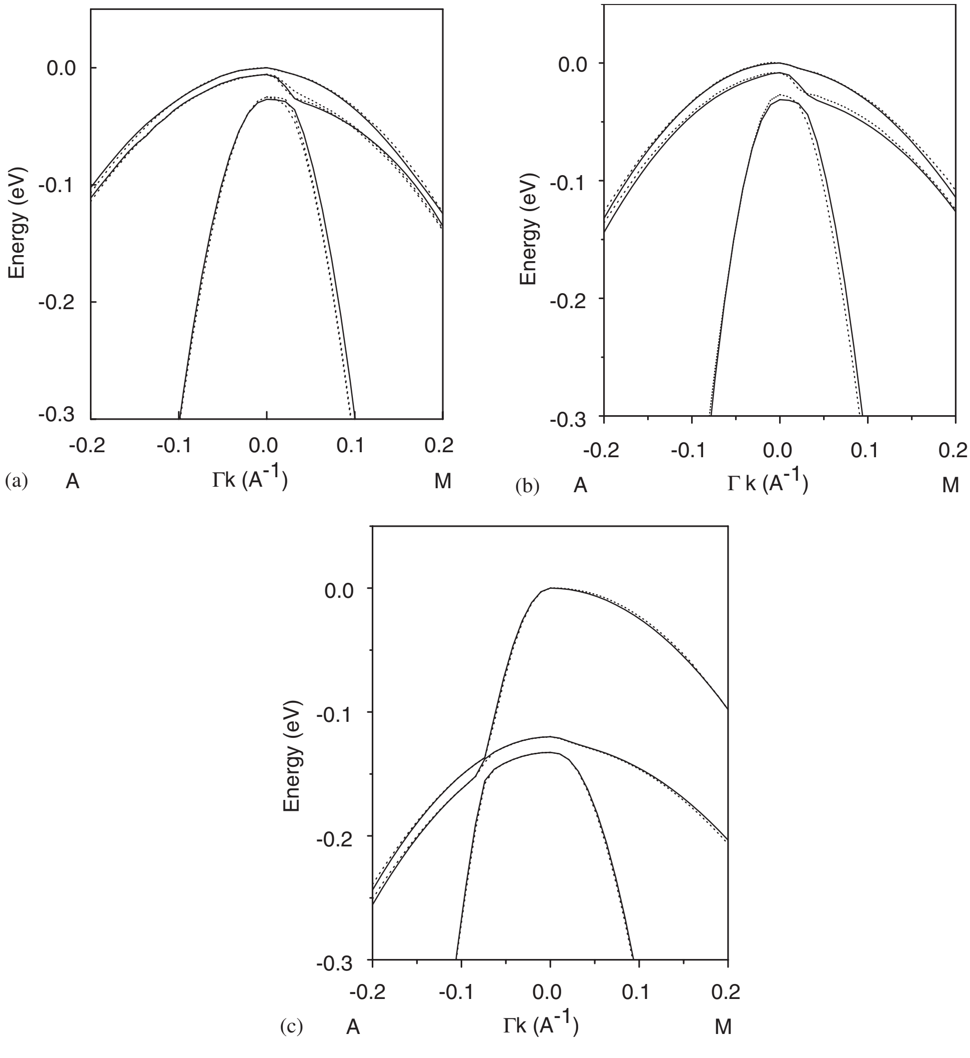

Fig. 4. The k.p (solid line) and EPM (dotted line) band structures for (a) GaN, (b) InN and (c) AlN at the Γ-point.

As the Luttinger-like parameters (A_i), and the valence and conduction band effective masses of wurtzite phase III-nitrides are useful for modeling the electronic structure and optical properties of simple heterostructure and devices, we make use of the effective-mass Hamiltonian in the cubic approximation to obtain these parameters [5]. In this approximation the valence band effective masses are related to A_i as in the following:

$$
\begin{aligned}
&\frac{1}{m^{\parallel}_{\mathrm{hh}}} = -(A_1 + A_3),\\
&\frac{1}{m^{\parallel}_{\mathrm{lh}}} = -(A_1 + A_3),\\
&\frac{1}{m^{\parallel}_{\mathrm{ch}}} = -A_1,\\
&\frac{1}{m^{\perp}_{\mathrm{hh}}} = -(A_2 + A_4 - A_5),\\
&\frac{1}{m^{\perp}_{\mathrm{lh}}} = -(A_2 + A_4 + A_5) - \frac{2A_7^2}{|\Delta_{\mathrm{cr}}|^2},\\
&\frac{1}{m^{\perp}_{\mathrm{ch}}} = -A_2 + \frac{2A_7}{|\Delta_{\mathrm{cr}}|^2},
\end{aligned}
\tag{6}
$$

where indices hh, lh and ch denote the heavy-hole, light-hole and crystal-field split-hole effective masses in units of the free electron mass, respectively. The quantity Δ_{cr} is the crystal-field splitting energy and the symbols $\perp$ and $\parallel$ denote the $\Gamma - M$ and $\Gamma - A$ directions, respectively. The values of A_i are determined by fitting the band edge dispersion by the k.p theory to that calculated by the EPM. To obtain the electron effective masses, a parabolic line fit has been used to the lowermost conduction band dispersion.

The values obtained for the A_i parameters and the effective masses of III-nitride semiconductors are shown in Tables 5 and 6, respectively. The value of A_7 for all structures has been assumed to be 0, as in previous works [5,32]. As it known from these tables, the results of our calculations are in good agreement with other published theoretical results.

The valence band structures using the parameters in Table 5 have been plotted for each of III-nitride materials using solid lines against the corresponding EPM results as dotted lines (Fig. 4). For each of material, there is generally good agreement between the k.p and semi-empirical band structures.

4. Conclusion

This work presents a detailed study of the electronic band structures of wurtzite GaN, InN and AlN by the EPM method. An analytical function for symmetric and antisymmetric parts of the pseudopotential with adjustable coefficients has been reported. The form of this potential is optimized through a fitting procedure in which we recursively calculate the band structures by comparing the calculated values of the energy gap, bandwidth, crystal-field splitting and effective masses with the experimental and recently published theoretical results.

Acknowledgments

The authors wish to thank Professor G.P. Srivastava from Exeter University, UK and Dr. S. Brand from Durham University, UK, for helpful discussions.

References

[1] K.C. Zeng, J.Y. Lin, H.X. Jiang, W. Yang, Appl. Phys. Lett. 74 (1999) 3821.
[2] D.C. Reynolds, D.C. Look, W. Kim, O. Aktas, A. Botchkarev, A. Salvador, H. Morkoc, D.N. Talwar, J. Appl. Phys. 80 (1996) 594.
[3] A. Asgari, M. Kalafi, L. Faraone, J. Appl. Phys. 95 (2004) 1185.
[4] A. Asgari, M. Kalafi, L. Faraone, Physica E 25 (2005) 431.
[5] M. Suzuki, T. Uenoyama, A. Yanase, Phys. Rev. B 52 (1995) 8132.
[6] M. Suzuki, T. Uenoyama, Jpn. J. Appl. Phys. 34 (Part 1) (1995) 3442.
[7] M.Z. Huang, W.Y. Ching, J. Phys. Chem. Solids 46 (1985) 977.
[8] K. Kim, W.R.L. Lambrecht, B. Segall, M.v. Schilfgaarde, Phys. Rev. B 56 (1997) 7363.
[9] A. Rubio, J.L. Corkill, M.L. Cohen, E.L. Shirley, St.G. Loui, Phys. Rev. B 48 (1993) 1810.
[10] M. Goano, E. Bellotti, E. Ghillino, G. Ghione, K.F. Brennan, J. Appl. Phys. 88 (2000) 6467.
[11] D.J. Dugdale, S. Brand, R.A. Abram, Phys. Rev. B 61 (2000) 12933.
[12] S.K. Pugh, D.J. Dugdale, S. Brand, R.A. Abram, Semicond. Sci. Technol. 14 (1999) 23.
[13] J.-B. Xia, K.W. Cheah, X.-L. Wang, D.-Z. Sun, M.-Y. Kong, Phys. Rev. B 59 (1999) 10119.
[14] Y.C. Yeo, T.C. Chong, M.F. Li, J. Appl. Phys. 83 (1998) 1429.
[15] D. Fritsch, H. Schmidt, M. Grundmann, Phys. Rev. B 67 (2003) 235205-1.
[16] M.L. Cohen, J.R. Chelikowsky, Electronic Structure and Optical Properties of Semiconductors, Springer, New York, 1989.
[17] H. Schulz, K.H. Thiemann, Solid State Commun. 23 (1977) 815.
[18] K. Osamura, S. Naka, Y. Murakami, J. Appl. Phys. 46 (1975) 3432.
[19] A.F. Wright, J.S. Nelson, Phys. Rev. B 51 (1995) 7866.
[20] S. Bloom, G. Harbecke, E. Meier, I.B. Ortenburger, Phys. Status Solidi B 66 (1974) 161.
[21] P. Perlin, I. Gorczyca, S. Porowski, T. Suski, N.E. Christensen, A. Polian, Jpn. J. Appl. Phys. 32 (1993) 334.
[22] B. Monemar, Phys. Rev. B 10 (1974) 676.
[23] R. Dingle, D.D. Sell, S.E. Stokowski, M. Ilegems, Phys. Rev. B 4 (1971) 1211.
[24] R.W. Hunt, L. Vanzetti, T. Castro, K.M. Chen, L. Sorba, P.I. Cohen, W. Gladfelter, J.M. Van Hove, J.N. Kuznia, M.A. Khan, A. Fransiosi, Physica B 185 (1993) 415.
[25] T.L. Tansley, C.P. Foley, J. Appl. Phys. 59 (1986) 3241.
[26] V.A. Tyagai, A.M. Evstigneev, A.N. Krasiko, A.F. Adreeva, V. Ya Malakhov, Sov. Phys. Semicond. 11 (1977) 1257.
[27] P.B. Perry, R.F. Rutz, Appl. Phys. Lett. 33 (1978) 319.
[28] L. Roskovcova, J. Pastrnak, Czech J. Phys. B 30 (1980) 586.
[29] M. Gautier, J.P. Duraud, C. Le Gressus, J. Appl. Phys. 61 (1994) 547.
[30] S. Bloom, T.K. Bergstresser, Solid State Commun. 6 (1968) 465.
[31] S.H. Wei, A. Zunger, Phys. Rev. B 69 (1996) 2719.
[32] S.L. Chuang, C.S. Chang, Phys. Rev. B 54 (1996) 2491.